The Unusual Structural Behavior of Heteroleptic Aryl Copper(I) Thiolato Molecules. Cis vs. Trans Structures and London Dispersion Effects

Wenxing Zou,[a] James C. Fettinger,[a] Petra Vasko,[b,*] Philip P. Power [a,*]

[a] Department of Chemistry, University of California, One Shields Avenue, Davis, California 95616, United States
[b] Department of Chemistry, University of Helsinki, P.O. Box 55, FI-00014, Finland

Supporting information

Table of Contents:

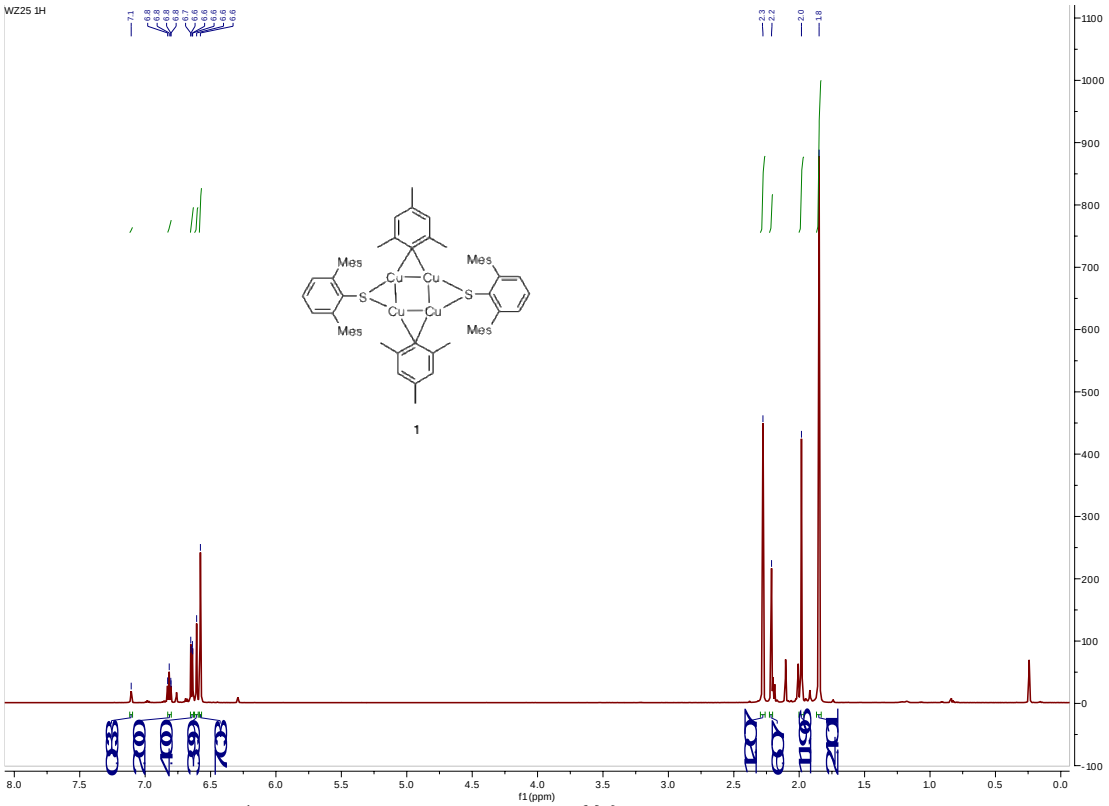

Figure S1. ^{1}H NMR spectrum of $\{Cu_2(SAr^{Me6})Mes\}_2$ (**1**) in C_6D_6 (600 MHz, 298 K)

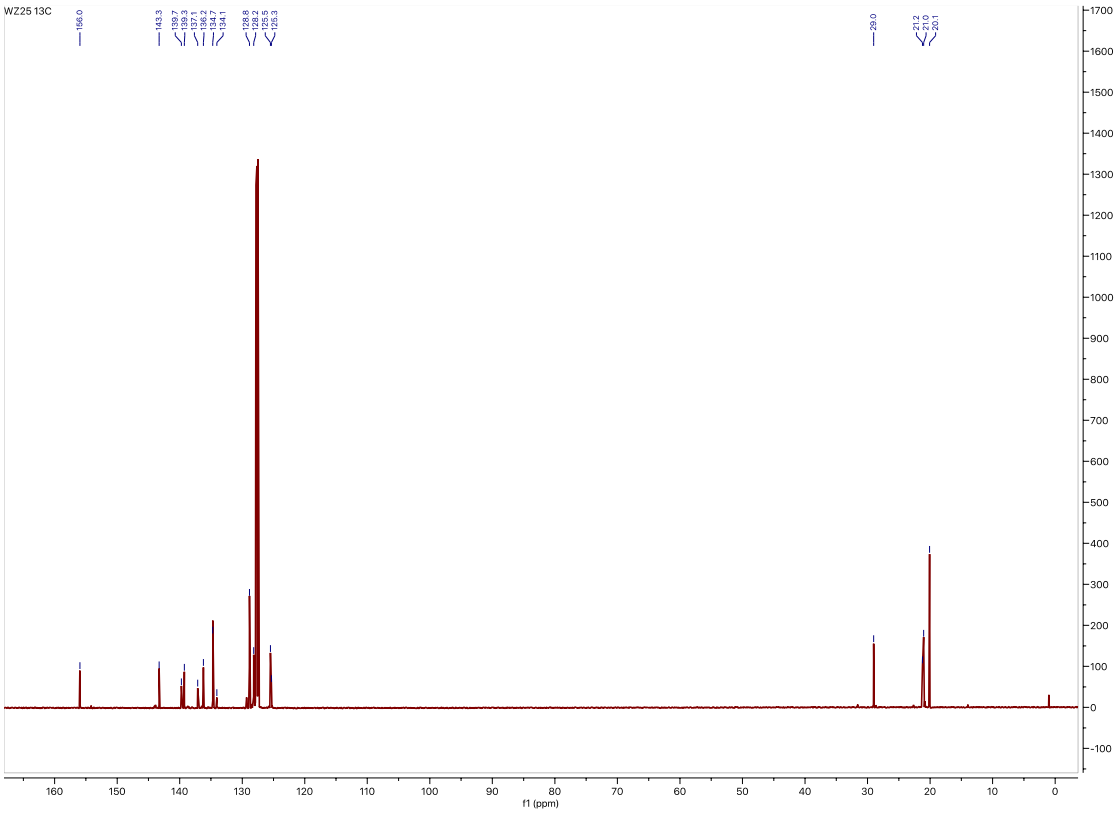

Figure S2. $^{13}C\{^{1}H\}$ NMR spectrum of $\{Cu_2(SAr^{Me6})Mes\}_2$ (**1**) in C_6D_6 (600 MHz, 298 K)

Figure S3. Infrared spectrum of a Nujol mull of $\{Cu_2(SAr^{Me6})Mes\}_2$ (**1**) at 25°C

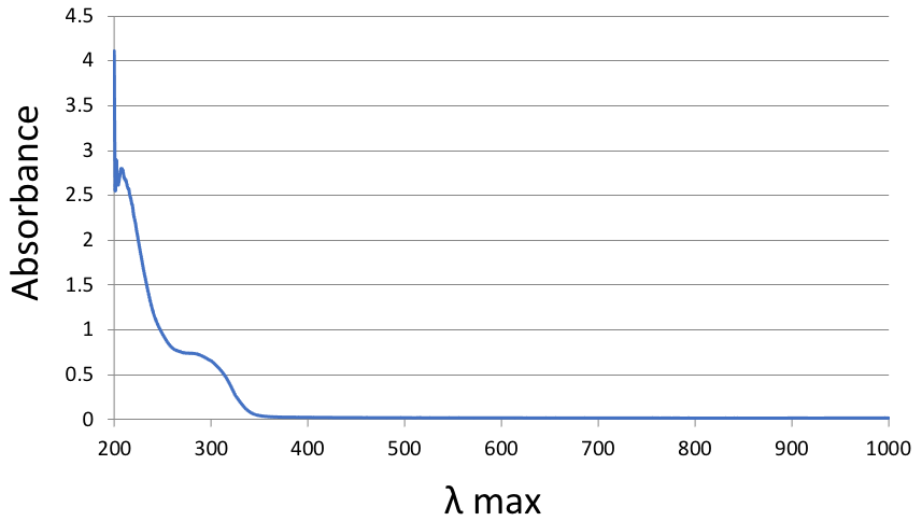

Figure S4. UV-Vis spectrum of $\{Cu_2(SAr^{Me6})Mes\}_2$ (**1**) at 25 °C (144 μM in hexanes)

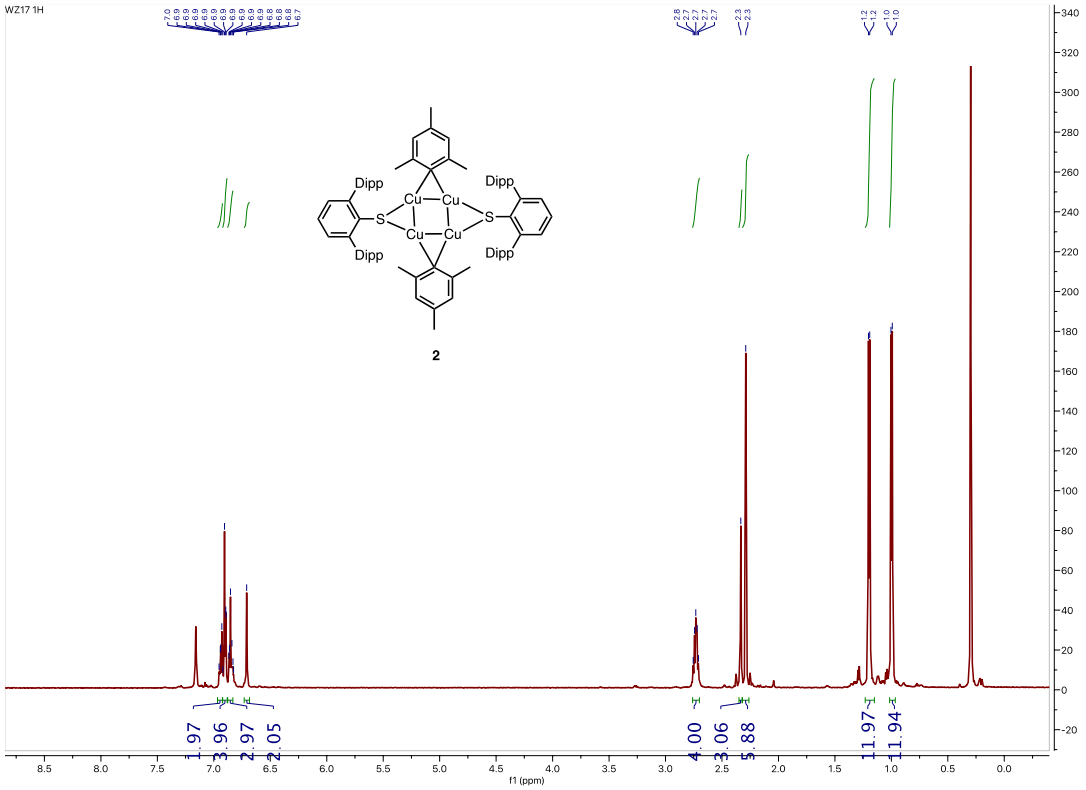

Figure S5. ^{1}H NMR spectrum of $\{Cu_2(SAr^{iPr4})Mes\}_2$ (**2**) in C_6D_6 (600 MHz, 298 K)

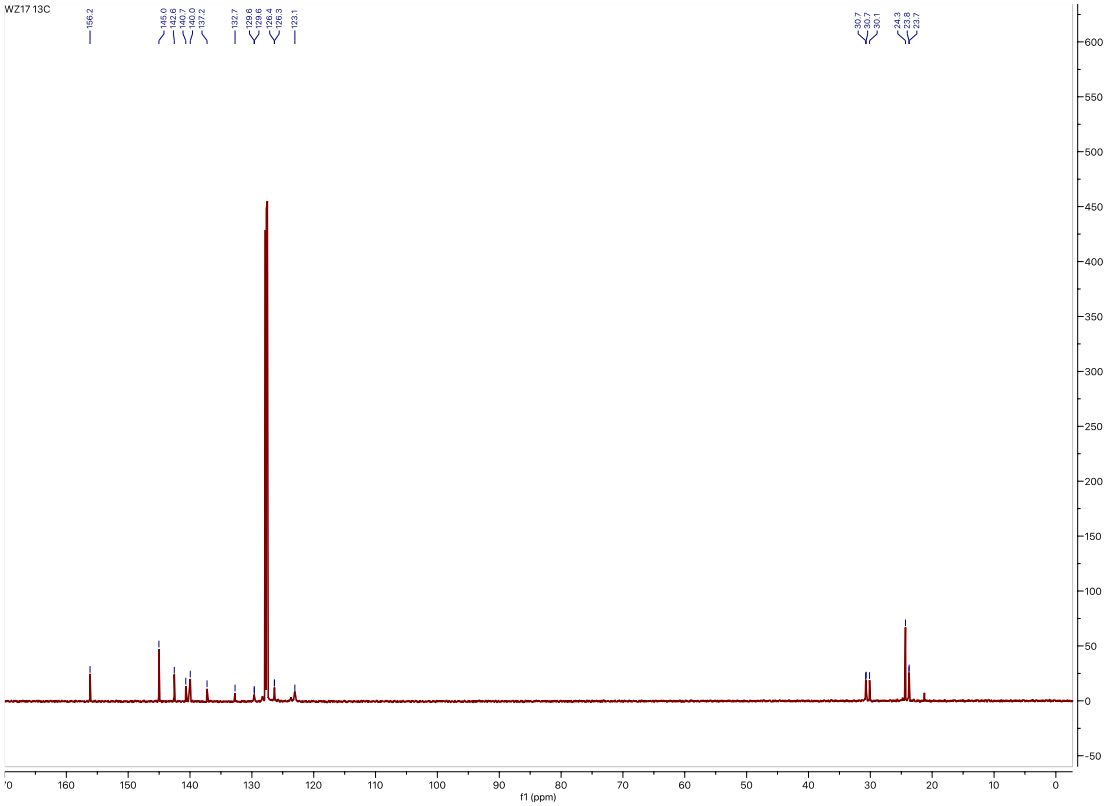

Figure S6. $^{13}C\{^{1}H\}$ NMR spectrum of $\{Cu_2(SAr^{iPr4})Mes\}_2$ (**2**) in C_6D_6 (150 MHz, 298 K)

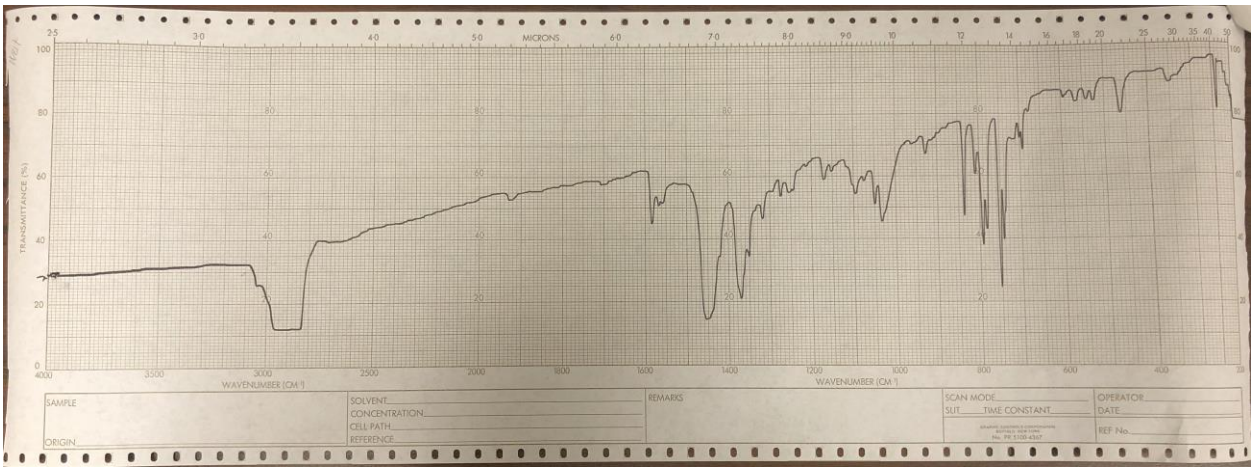

Figure S7. Infrared spectrum of a Nujol mull of $\{Cu_2(SAr^{iPr4})Mes\}_2$ (**2**) at 25°C

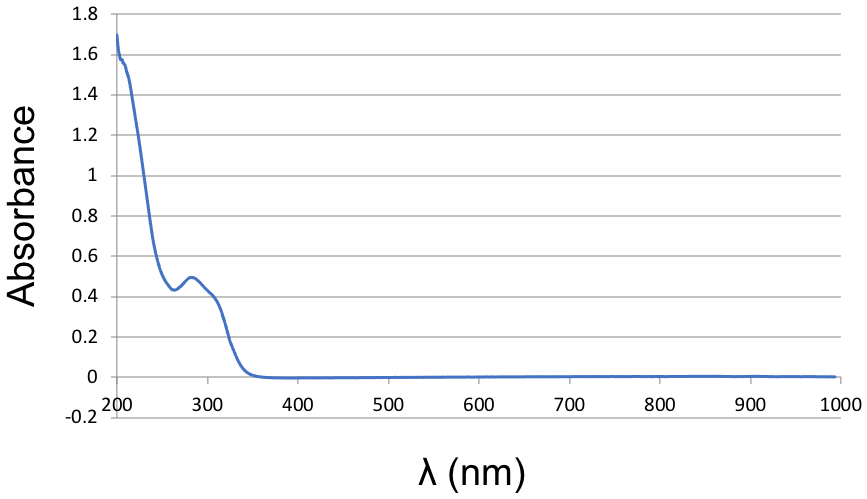

Figure S8. UV-Vis spectrum of $\{Cu_2(SAr^{iPr4})Mes\}_2$ (**2**) at 25 °C (163 µM in hexanes)

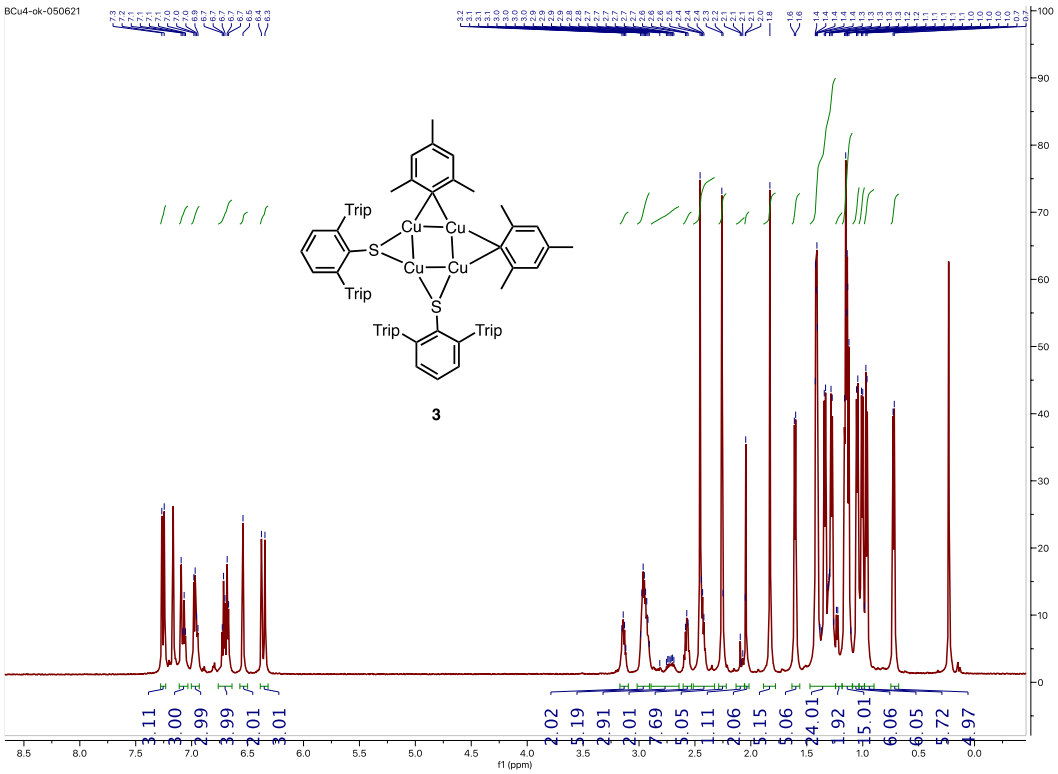

Figure S9. ^{1}H NMR spectrum of $\{Cu_2(SAr^{iPr6})Mes\}_2$ (**3**) in C_6D_6 (600 MHz, 298 K)

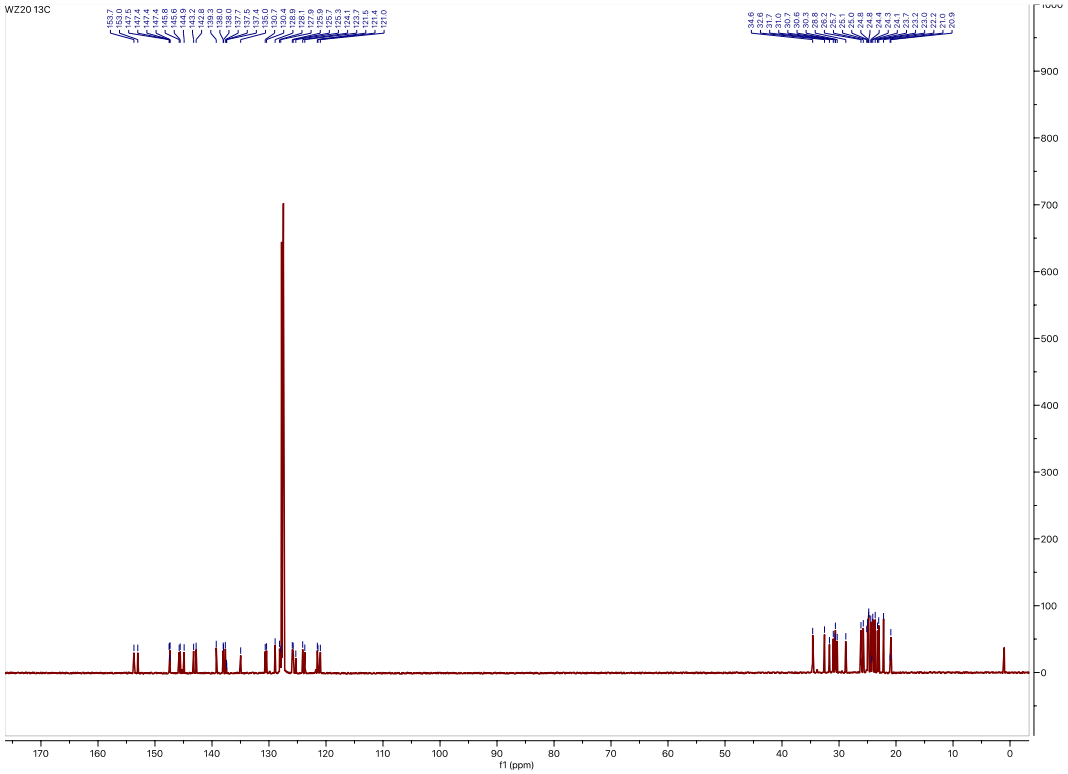

Figure S10. $^{13}C\{^{1}H\}$ NMR spectrum of $\{Cu_2(SAr^{iPr6})Mes\}_2$ (**3**) in C_6D_6 (150 MHz, 298 K)

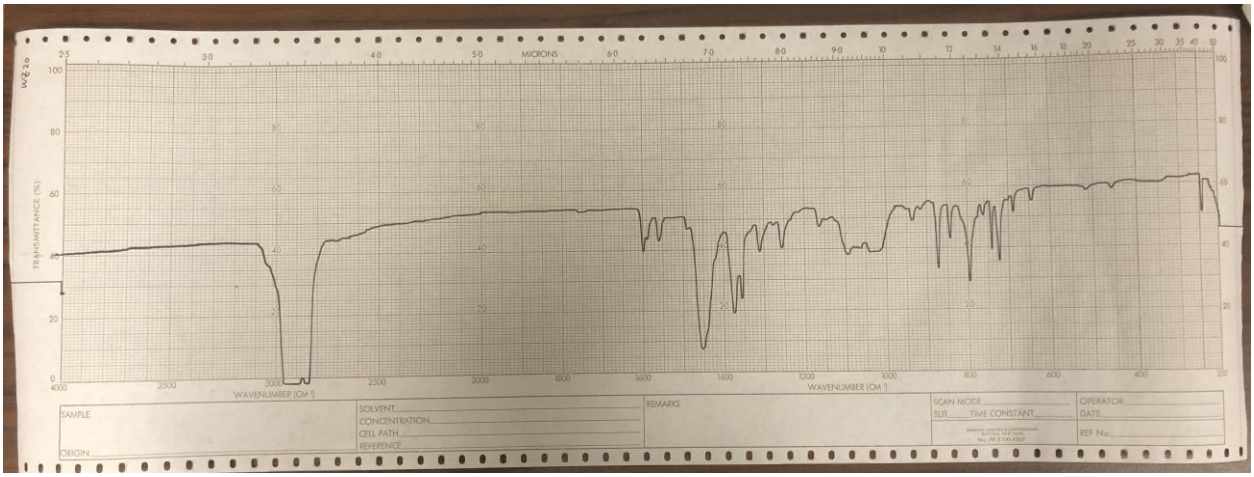

Figure S11. Infrared spectrum of a Nujol mull of $\{Cu_2(SAr^{iPr6})Mes\}_2$ (**3**) at 25°C

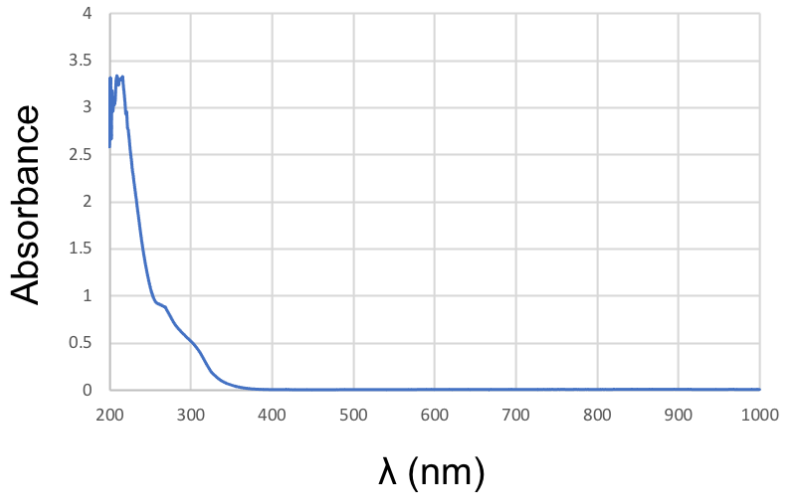

Figure S12. UV-Vis spectrum of $\{Cu_2(SAr^{iPr6})Mes\}_2$ (**3**) at 25 °C (279 μM in hexanes)

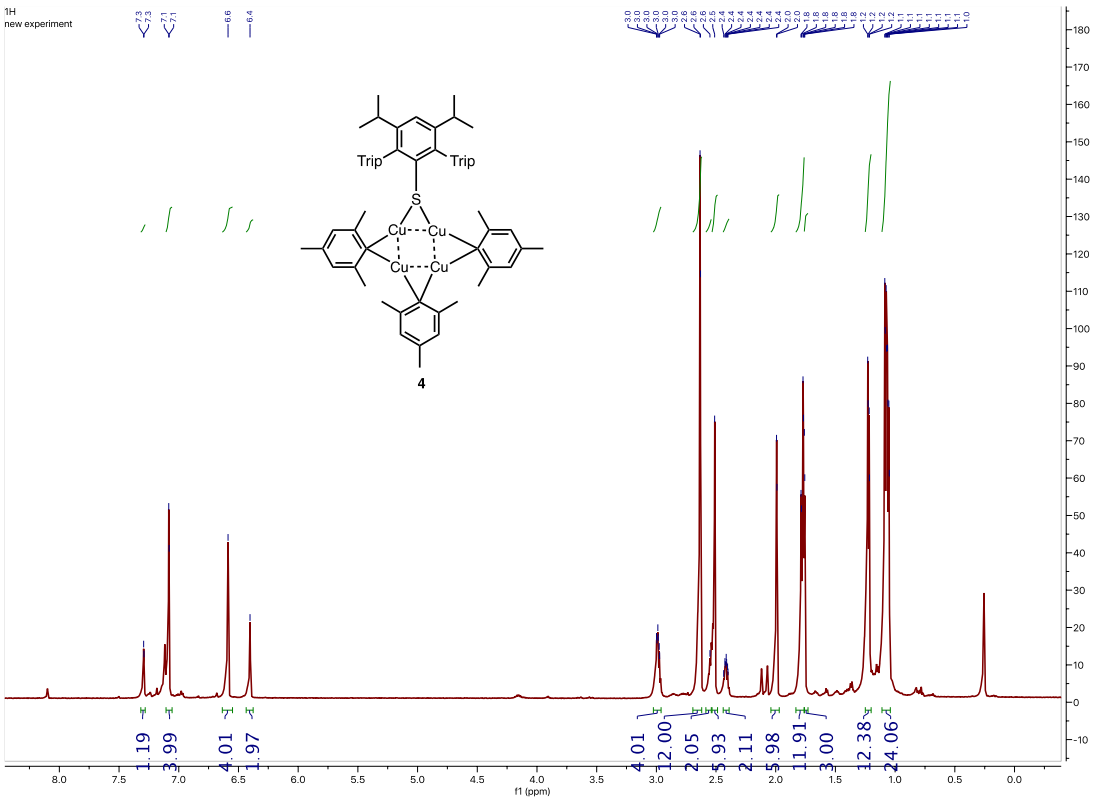

Figure S13. ^{1}H NMR spectrum of {$Cu_4(SAr^{iPr8})Mes_3$} (**4**) in C_6D_6 (600 MHz, 298 K)

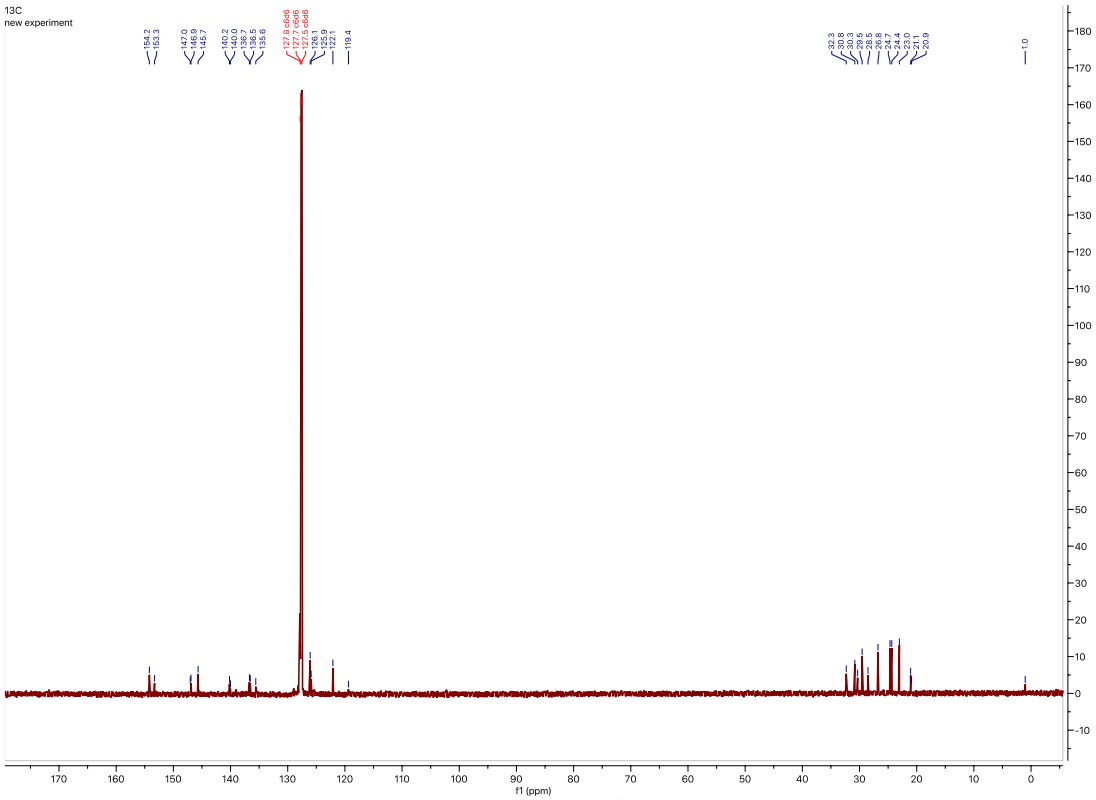

Figure S14. ^{13}C{^{1}H} NMR spectrum of {$Cu_4(SAr^{iPr8})Mes_3$} (**4**) in C_6D_6 (150 MHz, 298 K)

Figure S15. Infrared spectrum of a Nujol mull of {$Cu_4(SAr^{iPr8})Mes_3$} (**4**) at 25ºC

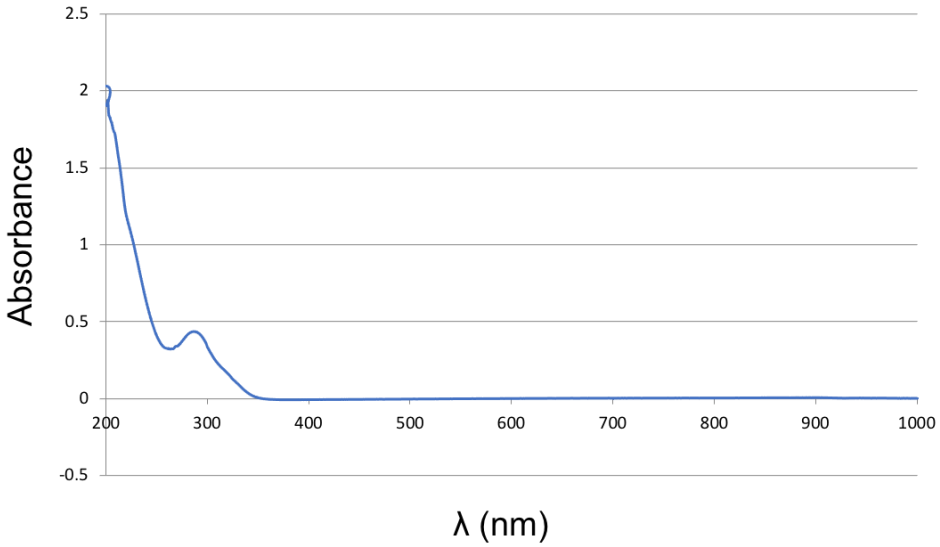

Figure S16. UV-Vis spectrum of {$Cu_4(SAr^{iPr8})Mes_3$} (**4**) at 25 °C (181 μM in hexanes)

Crystallography data

Table S1. Crystallographic parameters of **1-4**.

	1	**2**	**3**	**4**
formula	$C_{66}H_{72}Cu_4S_2$	$C_{78}H_{96}Cu_4S_2$	$C_{104}H_{136}Cu_4S_2$	$C_{69}H_{94}Cu_4S$
fw	1183.56	1351.82	1704.4	1209.70
color	colorless	colorless	colorless	colorless
cyst syst	monoclinic	monoclinic	triclinic	monoclinic
space group	C 2/c	P 2_1/n	P-1	P2_1/m
a, Å	25.0546(15)	12.6435(9)	15.6890(9)	12.1537(7)
b, Å	14.1816(9)	19.3995(17)	16.6057(10)	19.5933(12)
c, Å	32.2662(19)	14.6899(15)	18.1676(11)	14.0502(9)
α, deg	90	90	90.1316(10)	90
β, deg	96.6995(10)	108.793(9)	90.1437(10)	109.4542(9)
γ, deg	90	90	99.8453(10)	90
V, $Å^3$	11386.4(12)	3411.0(5)	4663.4(5)	3154.8(3)
Z	8	2	2	2
Density (calculated)	1.381 Mg/m^3	1.316 Mg/m^3	1.214 Mg/m^3	1.273 Mg/m^3
Absorption coefficient	1.587 mm^{-1}	2.281 mm^{-1}	0.989 mm^{-1}	1.401 mm^{-1}
F(000)	4928	1424	1816	1280
Crystal size	0.409 x 0.320 x 0.250 mm^3	0.476 x 0.371 x 0.267 mm^3	0.357 x 0.314 x 0.254 mm^3	0.368 x 0.237 x 0.232 mm^3
Crystal color and habit	Colorless Block	Colorless Block	Colorless Block	Colorless Block
Theta range for data collection	1.952 to 27.544°	3.911 to 69.613°	1.961 to 27.524°	2.079 to 27.547°
Index ranges	-32<=h<=32, -18<=k<=18, -41<=l<=41	-14<=h<=15, -23<=k<=22, -17<=l<=16	-20 <= h <= 20, -21 <= k <= 21, -23 <= l <= 23	-15<=h<=15, -25<=k<=25, -18<=l<=18

Reflections collected	50858	18204	42567	28803
Independent reflections	13126 [R(int) = 0.0493]	6264 [R(int) = 0.0208]	21444 [Rint = 0.0452]	7481 [R(int) = 0.0415]
Data / restraints / parameters	13126 / 0 / 667	6264 / 0 / 571	21444/0/1023	7481 / 0 / 366
Goodness-of-fit on F^2	1.031	1.053	1.021	1.030
Final R indices [I>2sigma(I)]	R_1 = 0.0332, wR_2 = 0.0732	R_1 = 0.0289, wR_2 = 0.0770	R_1 = 0.0410, wR_2 = 0.0829	R_1 = 0.0312, wR_2 = 0.0754
R indices (all data)	R_1 = 0.0493, wR_2 = 0.0792	R_1 = 0.0297, wR_2 = 0.0776	R_1 = 0.0663, wR_2 = 0.0917	R_1 = 0.0433, wR_2 = 0.0810
Largest diff. peak and hole	0.442 and -0.316 e.Å^{-3}	0.343 and -0.346 e.Å^{-3}	0.392 and -0.457 e.Å^{-3}	0.440 and -0.359 e.Å^{-3}

Computational details

Table S2. Optimized bond parameters of **2** and **3**.

	2 PBE1PBE-D3	**2** PBE1PBE	**3** PBE1PBE-D3	**3** PBE1PBE
Cu-Cu (Å)	2.465	2.509	2.433	2.463
	2.812	2.928	2.446	2.467
	2.466	2.509	2.701	2.800
	2.811	2.929	2.710	2.805
Cu-S (Å)	2.199	2.203	2.191	2.221
	2.202	2.208	2.232	2.215
Cu-C_{Mes} (Å)	2.003	2.005	2.022	2.013
	2.008	2.006	2.010	2.017
Cu-Cu-Cu (°)	77.15	83.43	71.97, 71.94	77.94, 77.92
	102.85	96.57	99.88, 116.17	93.00, 111.14
Cu-S-Cu (°)	79.40	83.21	75.28	78.29
Cu-C_{Mes}-Cu (°)	75.85	77.44	74.92	75.47
S-Cu-Cu-S/C (°)	66.52	50.56	16.03	5.90